Finite-lattice calculations for the two-dimensional axial-next-nearest-neighbor Ising model

G. O. Williams

Department of Physics, State University of New York at Albany, Albany, New York 12222

P. Ruján* and H. L. Frisch

Department of Chemistry, State University of New York at Albany, Albany, New York 12222
(Received 13 April 1981; revised manuscript received 17 August 1981)

The two-dimensional axial-next-nearest-neighbor Ising model is studied numerically using finite-lattice results. The row-to-row transfer matrix is mapped into a simple one-dimensional spin-$\frac{1}{2}$ quantum Hamiltonian. The leading eigenvalues and the corresponding eigenvectors are calculated numerically for chains of finite lengths. Using a finite-lattice renormalization-group transformation the high- (low-) temperature region is analyzed with the use of the Hamiltonian for the original (dual) model. Although there is no clear evidence for a massless phase, the phase boundaries obtained in this way are a strong indication of the presence of a sinusoidal phase between the paramagnetic and the $\langle 2 \rangle$ antiphase, in fair agreement with previous analytical results.

I. INTRODUCTION

Recently the two-dimensional ANNNI (axial-next-nearest-neighbor Ising model) has been intensively studied. Although invented by Elliott[1] in 1961 to describe the phase structure of rare-earth compounds, this model has also been proved to be related to the commensurate-incommensurate phase transitions and remains a challenging problem, both theoretically and experimentally.

The three-dimensional ANNNI model has an infinite number of phases and a very complex phase diagram,[2] shared by other models with competing interactions.[3] In two dimensions the model has been studied by Monte Carlo simulations,[4] by exactly soluble "mock" models,[5] and by an appropriate version of the Pokrovsky-Talapov[6,7] method. Recently one of us[8] has used exact mappings, high- and low-temperature expansions for the correlation length, and spin-wave approximations to obtain the critical behavior of the two-dimensional ANNNI model.

The phase diagram of the two-dimensional ANNNI model is shown in Fig. 1. The notation para indicates a paramagnetic phase which is of the usual type above the line $IL'D$, but which displays a strongly oscillatory behavior below this line. The notation ferro indicates a usual ferromagnetic phase, while the $\langle 2 \rangle$ phase is characterized by row configurations of two spins up, two spins down. The sinus phase is a genuine incommensurate phase with magnetization oscillating according to a characteristic wave vector. This type of phase diagram agrees with recent analytic calculations,[7-9] although some controversy still remains over the location of the Lifshitz point.[10]

In this paper we report the results of finite-lattice calculations. In interpreting the results one has to keep in mind that a true incommensurate phase appears only in the thermodynamic limit. Besides a quite accurate ferromagnetic-paramagnetic phase boundary, our main result is the suggestion of the existence of a "sinus" phase lying between the paramagnetic and the $\langle 2 \rangle$ phase, as indicated by the fact that the phase boundaries obtained by applying finite-size scaling[11] alternately to the original and dual models do not converge to a unique line.

Our paper is organized as follows. In Sec. II the model is defined, its row-to-row transfer matrix is
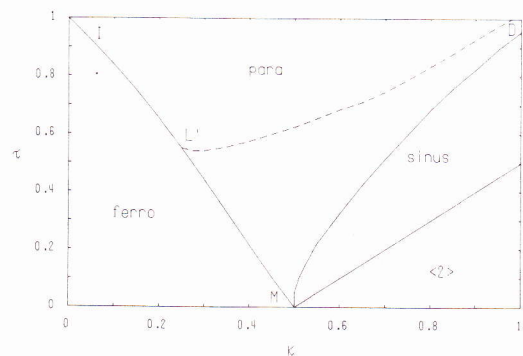

FIG. 1. The phase diagram of the two-dimensional ANNNI model. $\tau = K_{1y}^*/K_{1x}$ is the reduced temperature and $\kappa = |K_{2x}|/K_{1x}$ is the ratio of the competing interactions in the x direction. $I(\tau = 1, \kappa = 0)$ and $D(\tau = \kappa = \infty)$ are Ising critical points while $M(\tau = 0, \kappa = 0.5)$ is the multicritical point. For a discussion of the phases, see the text.

constructed and subsequently mapped into a one-dimensional quantum-spin Hamiltonian at $T=0$ in the so-called Hamiltonian limit. The dual of this Hamiltonian is also derived. The symmetries of these Hamiltonians, as well as our diagonalization procedure, are discussed. In Sec. III we present in graphical form the behavior of the leading eigenvalues of the different symmetry blocks for chains of eight spins. The finite-size scaling and the finite-lattice renormalization group transformations (FLRG) are presented in Sec. IV. The behavior of the (scaled) mass gaps (the mass gap is defined as the inverse of the correlation length) are presented in graphical form. Accordingly, the results obtained for the phase boundaries from the original and the dual Hamiltonian are discussed in Sec. V. They are compared to exact expansion results and previous analytic predictions. Although the mass gaps behave strangely in the region below the mean-field Lifshitz point ($\tau = K_{1y}^*/K_{1x} = \frac{3}{4}$, $K = |K_{2x}|/K_{1x} = \frac{1}{4}$), our numerical results support the form of the phase diagram first proposed by Villain and Bak[7] and by Coppersmith and coworkers,[9] namely, that the Lifshitz point is at $T=0$. Results for the critical exponents obtained from these methods are rather disparate. We have therefore applied a block-projection renormalization group method[12] (BPRG) to calculate the critical exponents. Although such methods lead to less accurate phase diagrams, the results obtained for the critical index of the correlation length are in keeping with expectations.

II. ANNNI MODEL

The two-dimensional ANNNI model is defined by

$$-\beta \mathcal{H} = \sum_{\vec{i}} (K_{1x} S_{\vec{i}} S_{\vec{i}+\vec{1}x} - |K_{2x}| S_{\vec{i}} S_{\vec{i}+\vec{2}x}$$

$$+ K_{1y} S_{\vec{i}} S_{\vec{i}+\vec{1}y}) \quad , \qquad (1.1)$$

where $\beta = 1/kT$, $\vec{i}$ runs over a square lattice and $\vec{1}x$, $\vec{1}y$ are unit vectors in the x, y directions, respectively. The variables $s_{\vec{i}}$ are usual Ising variables $s_{\vec{i}} = \pm 1$. The row-to-row transfer matrix V is given by

$$V = V_1 V_2 \quad , \qquad (1.2)$$

where V_1 represents the self energy of a row

$$V_1 = \prod_{i=1}^{N_C} \exp(K_{1x} \sigma_i^z \sigma_{i+1}^z - |K_{2x}| \sigma_i^z \sigma_{i+2}^z) \quad , \quad (1.3)$$

while V_2 contains the interrow interaction

$$V_2 = \prod_{i=1}^{N_C} C \exp(K_{1y}^* \sigma_i^x) \quad . \qquad (1.4)$$

Here $C = \exp(K_{1y}^*)/\cosh(K_{1y})$ is a constant and as

usual

$$K_{1y}^* = -\frac{1}{2} \ln \tanh K_{1y} \quad . \qquad (1.5)$$

The different symmetries of the model (1.1) and, correspondingly, of the operator (1.2) were discussed in detail in a previous paper.[8] Here we notice that in the so-called Hamiltonian limit, when K_{1x}, K_{2x}, and K_{1y}^* tend all to zero (but not the reduced temperature $\tau = K_{1y}^*/K_{1x}$, nor the competition ratio $\kappa = |K_{2x}|/K_{1x}$) the operator V goes to

$$V_H = C^{N_C} \left[1 + K_{1x} \sum_{i+1}^{N_C} (\sigma_i^z \sigma_{i+1}^z - \kappa \sigma_i^z \sigma_{i+2}^z + \tau \sigma_i^x) \right] \quad .$$

$$(1.6)$$

After neglecting the constants one is led to a linear $\frac{1}{2}$-spin Hamiltonian defined (after the canonical transformation $\sigma_i^x \leftrightarrow \sigma_i^z$) as

$$-H = \sum_i (\sigma_i^x \sigma_{i+1}^x - \kappa \sigma_i^x \sigma_{i+2}^x + \tau \sigma_i^z) \quad . \qquad (1.7)$$

The low-lying eigenvalues of this Hamiltonian correspond to the exponential of the largest eigenvalues of the transfer matrix. At $\kappa = 0$ the Hamiltonian (1.7) reduces to an Ising model in a transverse field. This model[13] is in the same universality class as the usual Ising model and the critical point is defined by $\tau_C = 1$. The same stands for $\tau, \kappa \gg 1$, where one recovers two independent Ising models in a transverse field situated on the even and the odd lattice points, respectively. At $\tau = 0$ one has an exactly soluble model, frozen into a ferromagnetic state if $\kappa < 0.5$ or a $\langle 2 \rangle$ state if $\kappa > 0.5$. .

Implementing the duality transformation through the bond operators

$$\mu_i^x = \sigma_i^z \sigma_{i+1}^z, \quad \mu_i^z = \prod_{j<i} \sigma_j^x \quad , \qquad (1.8)$$

the operator (1.6) will map after the canonical transformation $\mu_i^x \leftrightarrow \mu_i^z$ into the dual Hamiltonian H_D

$$-H_D = \sum_i (\mu_i^z - \kappa \mu_i^z \mu_{i+1}^z + \tau \mu_i^x \mu_{i+1}^x) \quad , \qquad (1.9)$$

which is an XZ (or XY) model in a longitudinal field. The duality transformation (1.8) "reverses" the magnitude of the temperature; accordingly, the paramagnetic region ($\tau \gg 1$) of the original model is mapped into a two-fold degenerate ferromagnetic state in the dual model (1.9). The ferromagnetic region of the original model corresponds to a disordered, paramagnetic phase in the dual model, while the $\langle 2 \rangle$ phase is mapped into a usual antiferromagnetic phase. These observations are important when interpreting the results of the finite-lattice calculations.

Finally let us mention that the (global) parity operator

$$P = \prod_i \sigma_i^z \qquad (1.10)$$

commutes with the Hamiltonians (1.7) and, in terms of μ_i's, (1.9). Therefore we have used a basis in which these Hamiltonians are automatically block diagonal and will use the label even (odd) to characterize eigenvalues corresponding to even (odd) eigenvectors. We shall additionally use the notation $k = 0$ ($\neq 0$) to label the eigenvalues of translationally invariant (non-invariant) states.

III. FINITE-LATTICE RESULTS

Using standard library routines we have exactly diagonalized the Hamiltonians (1.7) and (1.9) for chains of up to eight spins. A Lanczos tridiagonalization procedure,[14] for example, would allow the exact diagonalization of much larger lattices. However, by maintaining the spin basis in our calculations we are able to directly identify the spin configurations corresponding to the eigenvalues of the ground and first few excited states (we shall refer to these as leading eigenvalues). Moreover, the size dependence of the eigenvalues is quite smooth and we expect no surprises in their pattern for $N > 8$. Nonetheless, some tricks are necessary, especially in connection with the $\langle 2 \rangle$ phase of the original model.

It is worth mentioning that the duality transformation is strictly true only in the thermodynamic limit; for finite lattices one has to impose special boundary conditions.[8] However, for reasons of computational efficiency we have used periodic boundary conditions. In a few cases calculations have also been made with free boundary conditions and the correct boundary conditions; the results compare favorably with the results presented herein.

A. Original model

We have studied the leading eigenvalues of the even- and odd-symmetry blocks for $N = 3$, 4, 5, 6, 7, and 8. In order to account for the ground-state configurations ($\tau \sim 0$) one has to decline such lattices where the ground state would not fit, therefore if $\kappa > 0.5$ only chains comprising integral multiples of four spins are allowed.[15] We present here results for $N = 8$ which are typical for the pattern of the leading eigenvalues. In Figs. 2(a)−2(f) (the negative of) the lowest two eigenvalues of each symmetry block (even eigenvalues are full lines, while odd eigenvalues are dashed) are presented for $\kappa = 0$, 0.25, 0.4, 0.5, 0.7, and 1 as functions of the reduced temperature τ. The leading eigenstate of each block is translationally invariant but the second eigenstate is, in general, not.

For $\kappa < 0.5$ the ground state of the system is ferromagnetic and is twice degenerate at $\tau = 0$, consisting of even and odd translationally invariant eigenvectors, as it should. Therefore the mass gap showing the onset of ferromagnetism is just the difference between the corresponding eigenvalues. Let us point out that the critical temperature can be estimated quite well from the value of τ where the difference between the first and the second even eigenvalues is minimal (two full lines in the pictures). For example, $\tau_C = 1$ at $\kappa = 0$, as follows from self-duality arguments. The behavior of the odd eigenvalues at high temperatures is peculiar, especially for κ less than, but near 0.5, when they become degenerate at low temperature. This behavior indicates that the mass gap also has components which oscillate as a function of τ and κ [see Fig. 4(b) and also Sec. III B]. This is reflected in the rather peculiar behavior of the scaled mass gaps (see Sec. III B) for $\kappa \gtrsim 0.25$.

At $\kappa = 0.5$ all four eigenvalues are degenerate at $\tau = 0$ (many more eigenvalues, not shown here, are degenerate, too—for details see Ref. 16). The odd eigenvalues remain degenerate at any τ. As κ increases above 0.5, the four leading eigenstates remain degenerate at $\tau = 0$ as the $\langle 2 \rangle$ phase is four times degenerate. The odd eigenvalues are exactly degenerate for all values of τ, showing once more that the mass gap has an oscillating component (the second odd eigenvalue is not translationally invariant). As κ increases, so larger τ is needed to open the mass gap and in the κ, $\tau \rightarrow \infty$ limit one recovers an Ising-like picture.

B. Dual model

The same kind of "snapshot" is shown in Figs. 3(a)−3(f) for the dual model (1.9). Now the $\tau \sim 0$, $\kappa < 0.5$ is a paramagnetic region, where the even, $k = 0$, eigenvalue is unique. In the same region at large τ one enters into a ferromagnetic phase. This fact is very clear from the behavior shown in Figs. 3(a) and 3(b) and does not deserve any further comment. At $\kappa = 0.5$ the even and odd eigenvalues are degenerate in pairs. At $\tau = 0$ they are all degenerate, once more as a consequence of the high degeneracy of the multicritical point. As κ further increases a rather strange thing happens. At small τ the even eigenvalues are degenerate, a consequence of an antiferromagnetic ground state. Then the leading odd eigenvalue suddenly crosses both of them to become the ground-state energy to which the translationally invariant even eigenvalue tends from below in order to ensure the ferromagnetic behavior of the $\tau \gg 1$ phase. Strictly speaking, a crossing in the leading eigenvalue corresponds to a first-order phase transition. However, when using finite-size scaling a second-order transition takes place before the cross-
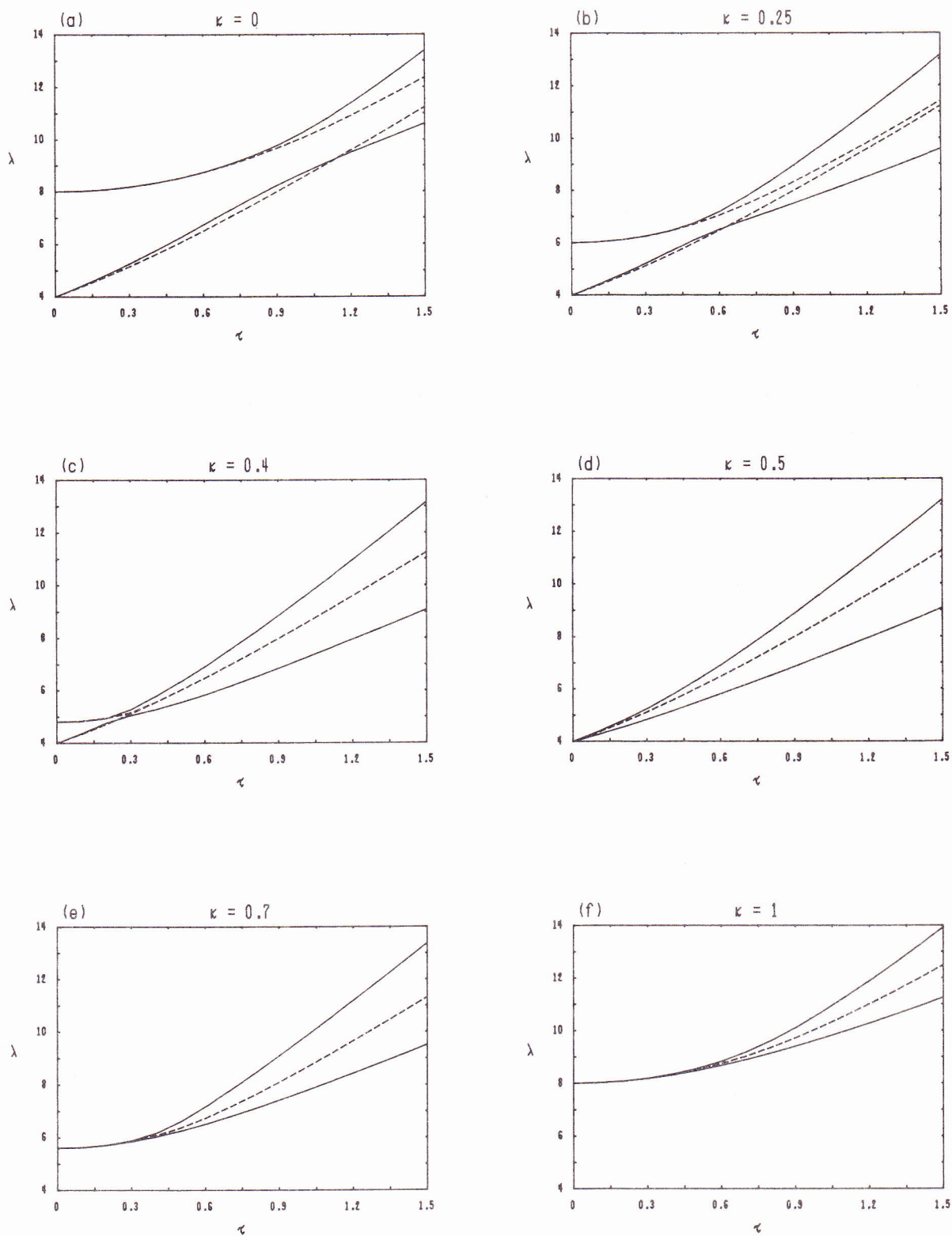
FIG. 2. The four leading eigenvalues of $-H$ (1.7) for the original model for a chain of eight spins for $\kappa = 0$, 0.4, 0.5, 0.7, and 1. The solid lines represent eigenvalues from the even-parity block while the dashed lines represent those from the odd-parity block.
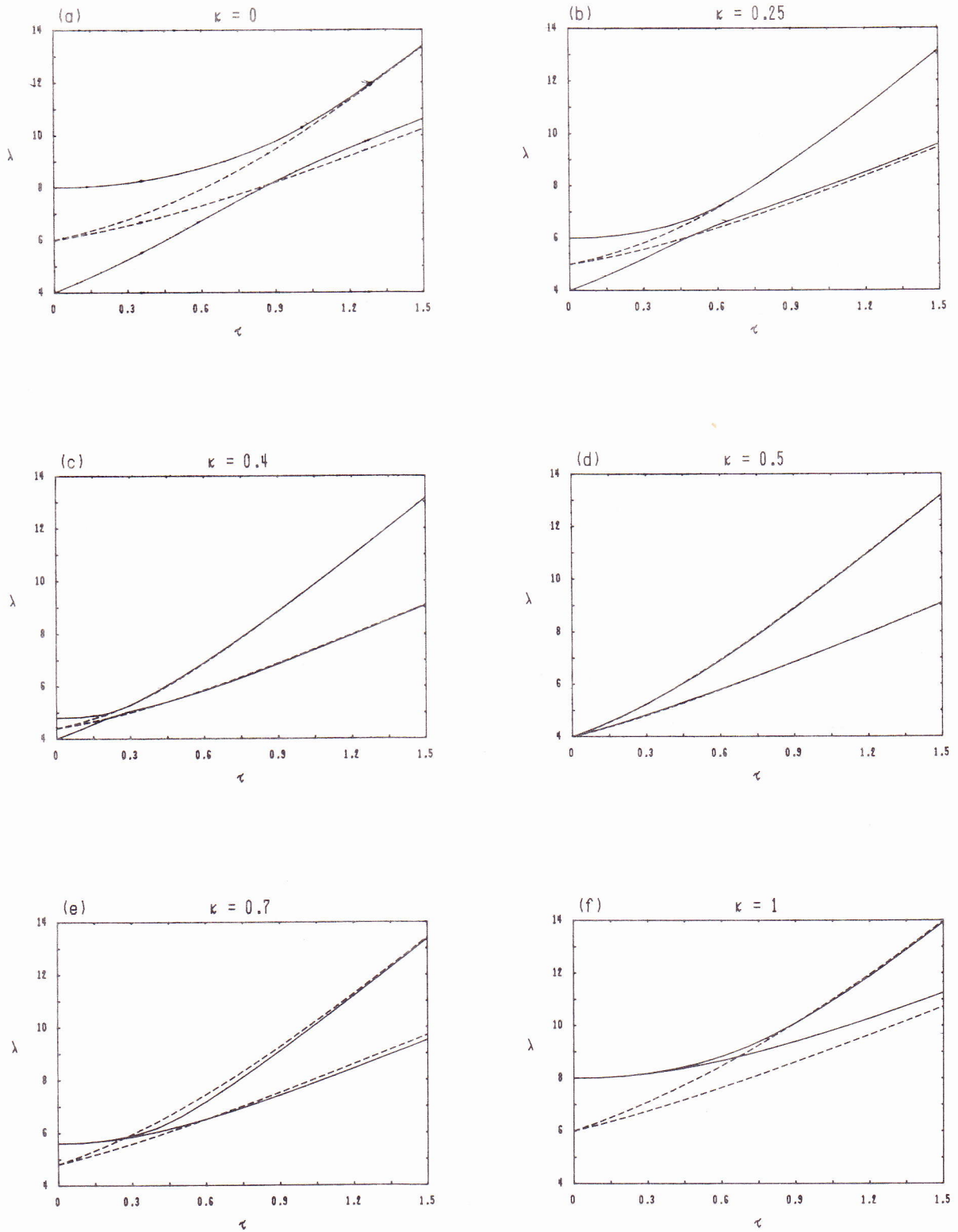
FIG. 3. The four leading eigenvalues of $-H_D$ (1.9) for the dual model for a chain of eight spins for $\kappa = 0$, 0.4, 0.5, 0.7, and 1. The solid lines represent eigenvalues from the even-parity block while the dashed lines represent those from the odd-parity block.

ing, which can indeed result in a rather large exponent for the specific heat.[17]

IV. FINITE-SIZE SCALING AND RENORMALIZATION GROUP

The basic concept of finite-size scaling can be expressed by postulating that the operator corresponding to finite-size effects has a critical index equal to one or, in other words, that if a thermodynamic quantity or other operator has in the thermodynamic limit a given singular behavior as a function of $|T - T_C|$, then for finite, but large, N its behavior can be parametrized by the same function of $1/N$ at the exact critical point

$$f(|T - T_C|) = f\left(\frac{1}{N}\right)\Bigg\|_{T = T_C} . \qquad (4.1)$$

This concept, introduced as early as 1941[18] and later developed and generalized by Fisher and Barber,[19] has proved to be a very useful tool in evaluating critical behavior from machine-experiment results.

The finite-lattice renormalization group transformations can be classified into basically two groups. One group uses the original ideas of Kadanoff[20] and Wilson[21] as implemented by Niemeijer and van Leeuwen[22] and we will call them block-spin methods. These methods use perturbation theory[23] or a projection technique in order to reduce the number of degrees of freedom.[24] A different method, first applied to the transfer matrix by Nightingale[11] and used in the context of quantum-spin systems by different groups,[25] is a direct implementation of the finite-size scaling idea. It considers the correlation length (or its inverse, the mass gap) as the basic quantity and it assumes that for sufficiently large $N' > N$

$$N\Delta_N(\tau, \kappa) = N'\Delta_{N'}(\tau', \kappa) , \qquad (4.2)$$

defining implicitly a unique relationship between the original and renormalized temperatures, τ and τ', respectively. The fixed point (critical temperature) is obtained from

$$N\Delta_N(\tau_C, \kappa) = N'\Delta_{N'}(\tau_C, \kappa) , \qquad (4.3)$$

while the critical exponent y_τ is derived as usual[22] to be

$$y_T = \frac{\partial N\Delta_N(\tau, \kappa)}{\partial \tau} \bigg/ \frac{\partial N'\Delta_{N'}(\tau', \kappa)}{\partial \tau'} \bigg|_{\tau = \tau' = \tau_C(N, N')} . \qquad (4.4)$$

We have applied this method throughout the paper in view of the reliable results it gives for quite different models and different types of critical behavior.[26]

The method works best when N and N' are chosen

as close to each other as possible without changing the nature of the ground state. A critical point obtained in this way will be denoted by $\tau_C(N,N')$ and the thermal critical exponent by $y_T(N,N')$. Using increasingly large values of N one can extrapolate the series of results to obtain very accurate values.[11] In the original model N and N' must be multiples of four when $\kappa > 0.5$, as discussed earlier. Therefore we can use only a $4 \to 8$ mapping from our finite-lattice results and we have no information on the convergence of this result.

In Figs. 4(a) and 4(b) are presented the scaled mass gaps $N\Delta_N(\tau, \kappa)$ of the original Hamiltonian versus the scaled temperature τ for $\kappa = 0$ and $\kappa = 0.4$. For $\kappa = 0$ (Ising model) the mass gaps behave as expected, with a very clean intersection near $\tau = 1$. As κ increases, the points of intersection move to smaller values of τ. At $\kappa = 0.5$, the scaled mass gaps vanish at $\tau = 0$, independently of N. In Figs. 5(a)−5(d) the scaled mass gaps of the dual Hamiltonian are shown for $\kappa = 0$, 0.4, 0.7, and 1. The behavior shown is in keeping with that of the original model and indicates clearly the convergence of the method. Note that the vanishing of the mass gaps as $\tau \to 0$ in the original model corresponds to the degeneracy of the ground state. Similarly, the mass gaps in the dual
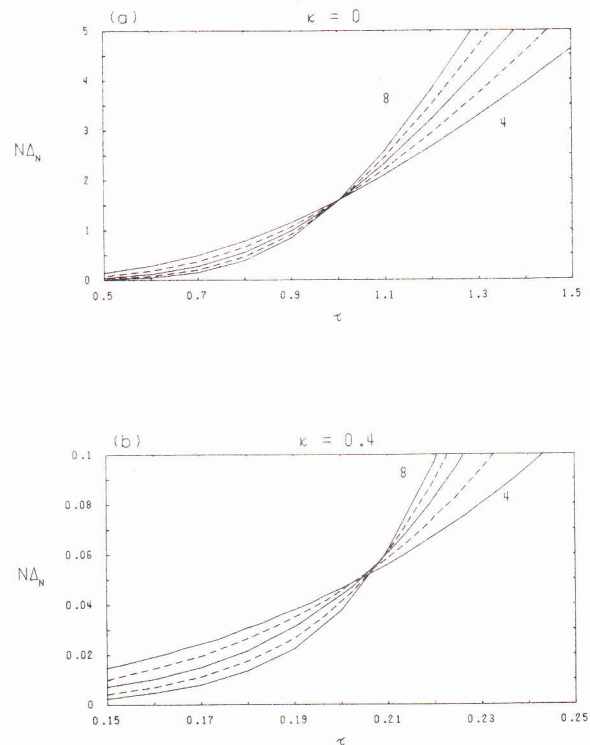

FIG. 4. The scaled mass gaps $N\Delta_N(\tau)$ for $\kappa = 0$ and $\kappa = 0.4$ in the original model. The points of intersection yield the critical points $\tau_C(N, N+1)$, $N = 4, 5, 6, 7$. Some curves are dashed as a visual aid.
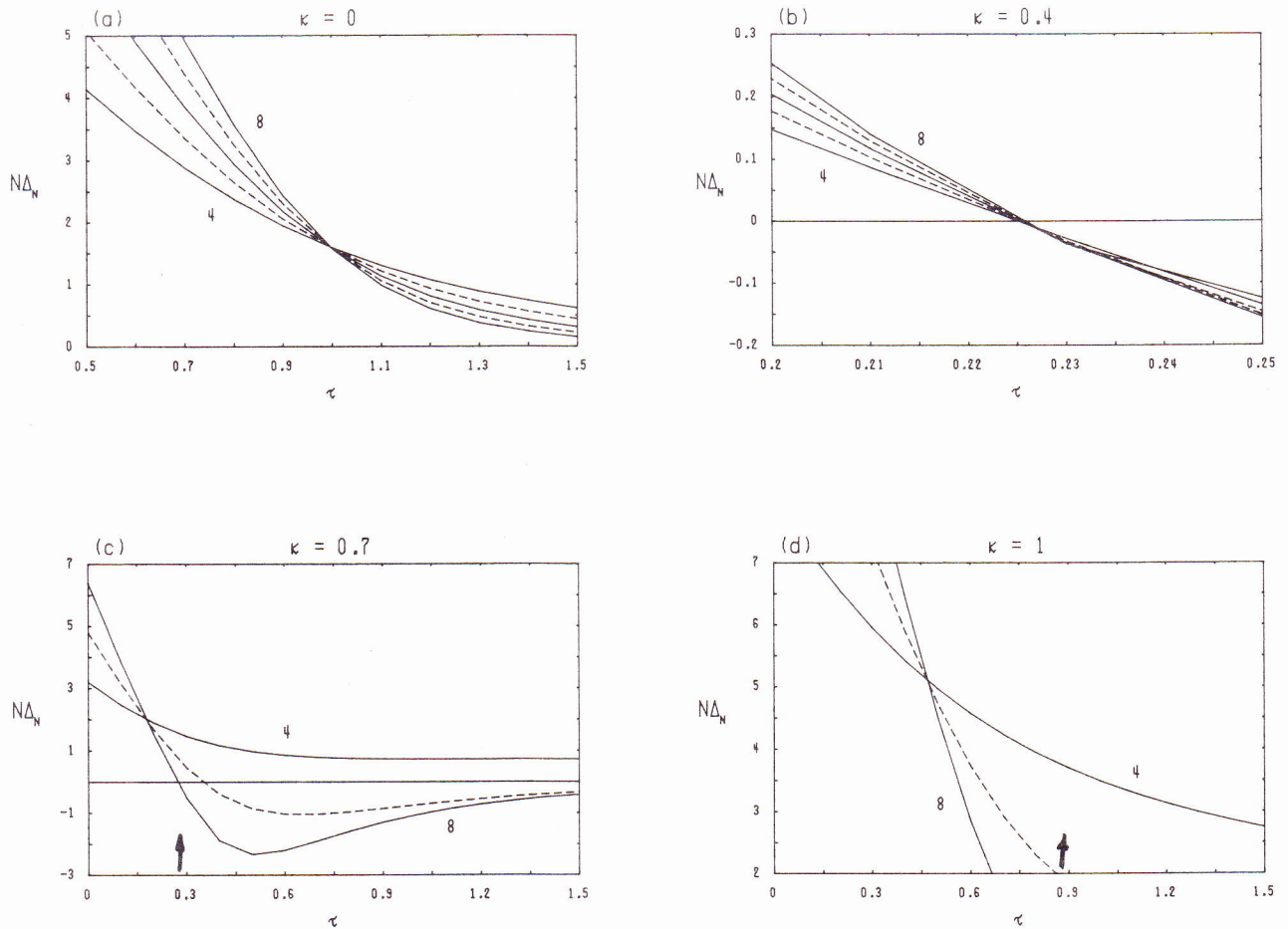
FIG. 5. The scaled mass gaps $N\Delta_N(\tau)$ for $\kappa = 0$, 0.4, 0.7, and 1 in the dual model. The arrows in (c) and (d) indicate the crossings occurring in the ground state which correspond to a first-order phase transition [see Figs. 3(e) and 3(f)]. Some curves are dashed as a visual aid.

model must tend asymptotically to zero as now the high-temperature state ($\tau \rightarrow \infty$) of the dual model is ferromagnetic; this tendency is evident in Fig. 5(c) (dual model, $\kappa = 0.7$).

It has been pointed out[14] that the FLRG techniques are not reliable after the first crossing in the mass gaps. However, a peculiar behavior observed at temperatures above the critical temperature may suggest the presence of an oscillatory phase. Shown respectively in Figs. 6(a) and 6(b) are the scaled mass gaps of the original and dual Hamiltonians for $\kappa = 0.4$. Visible in the original model are a series of crossings associated with a change in slope of the scaled mass gaps. This behavior, which becomes more prominent as N increases, becomes apparent at $\kappa \gtrsim 0.25$ and persists through $\kappa = 0.5$. Such additional crossings are visible for $\kappa > 0.5$; however they appear only for large N and move rapidly toward large τ as κ increases above 0.5. In the dual model, one also

observes additional crossings which first appear at $\kappa \gtrsim 0.25$, but there is no direct correspondence with the behavior observed in the original model. We attribute this anomalous behavior in both cases, however, to the strong oscillations of the spin-spin correlations expected in this region of the phase diagram. Note that a negative mass gap implies that the ground state comes from the odd symmetry block as may be seen from Figs. 3(e) and 3(f).

V. CONCLUSIONS

By a rigorous mathematical fitting procedure[11] one may estimate $\tau_C(\kappa) = \lim_{N,N'} \tau_C(N,N',\kappa)$ with reasonable confidence. Presented in Fig. 7 for $\kappa < 0.5$ are $\tau_C(N,N+1)$ for $N = 4, 5, 6$, and 7 for the original model. The convergence of the method is
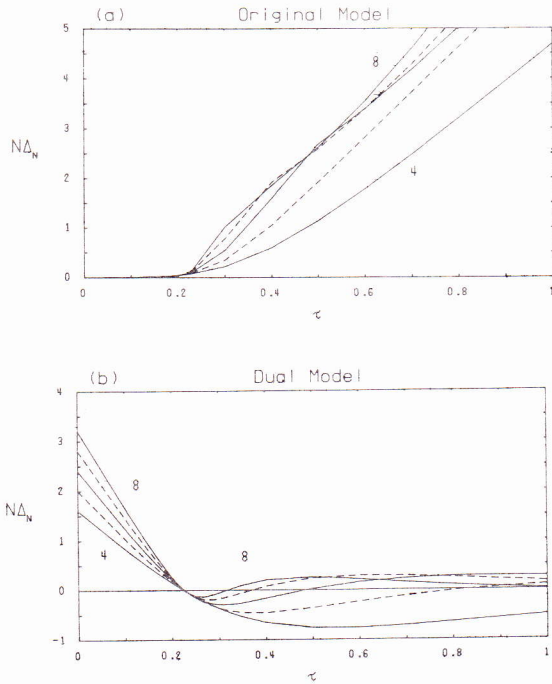
(a) Original Model

(b) Dual Model

FIG. 6. Scaled mass gaps for $\kappa = 0.4$ in the original and dual models. Besides the well-defined crossings at small τ defining the ferromagnetic $\rightarrow$ paramagnetic and paramagnetic $\rightarrow$ ferromagnetic phase transitions, note the peculiar series of additional crossings at higher temperatures which, in our opinion, are due to gap oscillations unrelated to the critical behavior. Some curves are dashed as a visual aid.

apparent, as comparison at $\kappa = 0$ of $\tau_C(7, 8) = 1.001$ with the exact value of 1 indicates. For $\kappa > 0.5$, we have only a single result, as indicated above. However, we expect $\tau_C(4, 8)$ to be in error by at most a few percent over the interval shown. The phase diagram obtained by the block-projection renormalization
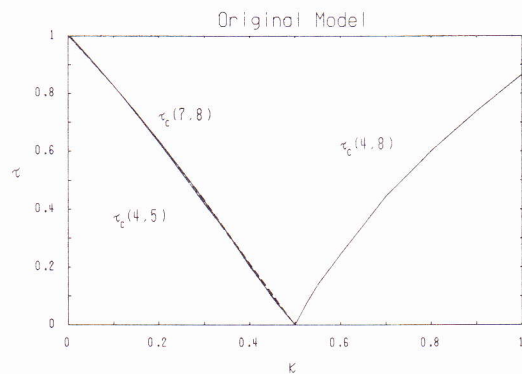

Original Model

FIG. 7. $\tau_C(N, N+1)$ for $N = 4$, 5, 6, and 7 ($\kappa < 0.5$) and $\tau_C(4, 8)$ for $\kappa > 0.5$ as obtained from the original model (1.7). Note the obvious convergence of the method for $\kappa < 0.5$.
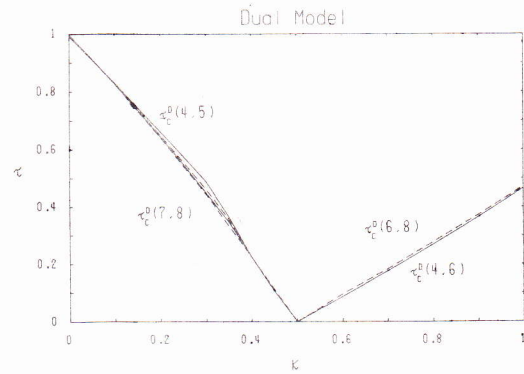

Dual Model

FIG. 8. $\tau_C^D(N, N+1)$ for $N = 4$, 5, 6, and 7 ($\kappa < 0.5$) and $\tau_C^D(N, N+2)$ for $N = 4$ and $N = 6$ as obtained from the dual model (1.9). Once again, note the convergence of the method.

group method[12] mentioned in Sec. I agrees quantitatively with these results around $\kappa = 0.5$ and retains a qualitative agreement everywhere.

Our results for the dual model are presented in Fig. 8. For $\kappa < 0.5$ are shown $\tau_C^D(N, N+1)$ for $N = 4$, 5, 6, and 7. The convergence is comparable to that obtained in the original model; at $\kappa = 0$, $\tau_C^D(7, 8)$ $= 0.999$. For $\kappa > 0.5$ we are able to make calculations for chains of 4, 6, and 8 spins. The agreement between $\tau_C^D(4, 6)$ and $\tau_C^D(6, 8)$ is indicative of rapid convergence.

In Fig. 9 we summarize our results. The original and dual models must perforce have the same phase diagrams, although our studies cannot produce the entire phase diagram from either model alone.[14] The obvious agreement of the original and dual models for $\kappa < 0.5$ clearly defines the phase boundary between the low-temperature ferromagnetic state (I)
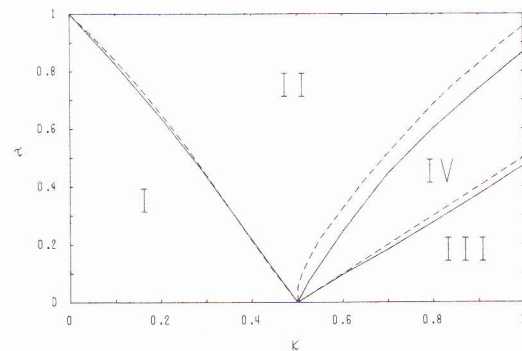

FIG. 9. The phase diagram obtained from Figs. 7 and 8 (full lines). The phase boundary I-II is compared to second-order perturbation-theory results; the boundary III-IV is compared to first-order perturbation-theory results; the boundary II-IV is compared to a low-temperature spin-wave approximation (Ref. 8).
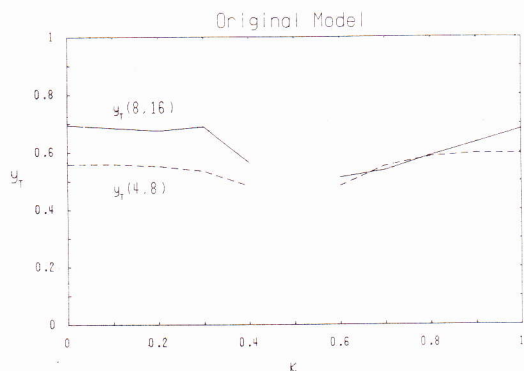
FIG. 10. The thermal index y_T as determined by the BPRG method for the original model. For $\kappa > 0.5$, y_T is determined at the phase boundary II → IV (paramagnetic → sinus).

FIG. 11. The thermal index y_T as determined by the FLRG method for the dual model. For $\kappa > 0.5$, y_T is determined at the phase boundary III → IV ($\langle 2 \rangle$ → sinus).

and the high-temperature paramagnetic state (II). The phase boundary plotted here is the average of $\tau_C(7, 8)$ and $\tau_C^D(7, 8)$. Shown for comparison is the second-order low-temperature perturbation-theory result (dashed curve).

For $\kappa > 0.5$, the situation is not as clear. Shown in Fig. 9 are $\tau_C(4, 8)$ (upper curve) and $\tau_C^D(6, 8)$. The convergence of the FLRG method for the dual model has been demonstrated, albeit by only two points of the sequence. The dashed line above $\tau_C^D(6, 8)$ is a first-order low-temperature perturbation-theory result and indicates that this phase boundary is correct at low temperature. The single curve $\tau_C(4, 8)$ obtained by FLRG methods, substantiated by the BPRG method, is further supported by numerical calculations of a spin-wave approximation valid at low temperature (dashed curve). Since the results of finite scaling are not valid beyond the first crossing in the mass gaps, we do not expect to observe the entire phase diagram in either model. These results indicate that a fourth phase (IV) must be sandwiched by the low-temperature $\langle 2 \rangle$ phase (III) and the high-temperature paramagnetic phase (II). We believe the phase IV to be the incommensurate phase whose potential existence has stimulated most of the recent investigations of the two-dimensional ANNNI model.

The nature of the phase transitions in this model are also of interest. We have studied the thermal critical index y_T for both models. The ferromagnetic-paramagnetic phase transition is most likely of Ising type. Results for y_T from the BPRG technique as applied to the original model are shown in Fig. 10 and those from the FLRG, as applied to
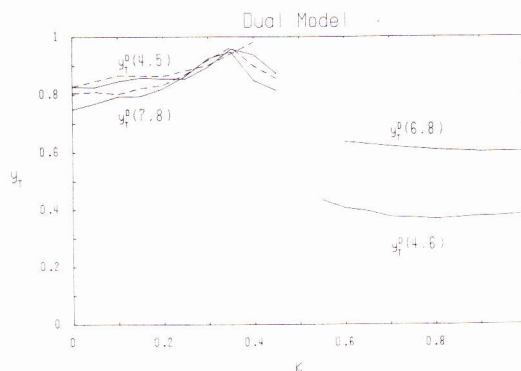
the dual model, in Fig. 11. Although neither method reproduces the exact result of $y_T(\kappa = 0) = 1$, it is probable that y_T is a constant for $\kappa < 0.5$. For $\kappa > 0.5$, it seems that the transition II → IV is more complicated, while our results on the transition III → IV are inconclusive. We obtain no information on the transitions IV → II and IV → III. It has been suggested that as one approaches the boundary III-IV from below, the behavior of the model is regular ($\alpha = 0$), while from above $\alpha = \frac{1}{2}$.[27] At the phase boundary $\eta = \frac{1}{8}$.[7,27] Along the boundary II-IV, $\eta^D = 1$.[8] Although our methods have shown that the phase diagram can be generated from relatively short chains of spins, it is apparent that the critical behavior of the infinite chain, as specified by the critical indices, is not attained in such short chains.

In conclusion, it is apparent that simple Ising models with competing interactions provide models with commensurate-incommensurate phase transitions which can be easily studied by a variety of methods, including Monte Carlo methods, various renormalization group techniques, and exact calculations. Such models might well provide a proving ground for theories of melting in two dimensions.

ACKNOWLEDGMENTS

*On leave from Institute for Theoretical Physics, Eötvös University, Puskin u. 5-7, Budapest 1088, Hungary.

[1] R. J. Elliott, Phys. Rev. <u>124</u>, 346 (1961).

[2] P. Bak and F. van Beohm, Phys. Rev. B <u>21</u>, 5297 (1980); J. Villain and M. B. Gordon, J. Phys. C <u>13</u>, 3117 (1980); M. E. Fisher and W. Selke, Phys. Rev. Lett. <u>44</u>, 1502 (1980); Philos. Trans. R. Soc. (in press).

[3] W. Selke, J. Phys. C <u>14</u>, L17 (1981).

[4] R. M. Hornreich, R. Liebmann, H. G. Schuster, and W. Selke, Z. Phys. B <u>35</u>, 91 (1979); W. Selke and M. E. Fisher, *ibid.* <u>40</u>, 71 (1980).

[5] D. A. Huse, M. E. Fisher, and J. M. Yeomans, Phys. Rev. B <u>23</u>, 180 (1981).

[6] V. L. Pokrovsky and A. L. Talapov, Phys. Rev. Lett. <u>42</u>, 65 (1979).

[7] J. Villain and P. Bak, J. Phys. (Paris) (in press).

[8] P. Ruján, Phys. Rev. B <u>24</u>, 6620 (1981).

[9] S. N. Coppersmith, D. S. Fisher, B. I. Halperin, P. A. Lee, and W. F. Brinkmann, Phys. Rev. Lett. <u>46</u>, 549 (1981).

[10] Monte Carlo calculations (Ref. 4) and high-temperature expansions (Ref. 8) seem to indicate a finite-temperature Lifshitz point while low-temperature spin-wave approximations (Refs. 7–9) show that it is at $\tau = 0$ (see Ref. 8 for a discussion).

[11] M. P. Nightingale, Physica (Utrecht) <u>83A</u>, 561 (1976); Phys. Lett. <u>59A</u>, 486 (1977).

[12] Method II of R. Julline, J. N. Fields, and S. Doniach, Phys. Rev. B <u>16</u>, 4889 (1977), has been applied to calculate the low-lying spectrum of finite chains of 8, 16, and 32 spins. The results were used in the context of Eqs. (4.2)–(4.4).

[13] P. Pfeuty, Ann. Phys. (N.Y.) <u>57</u>, 79 (1970).

[14] H. H. Roomany, H. W. Wyld, and L. E. Holloway, Phys. Rev. D <u>21</u>, 1557 (1980).

[15] According to the interpretation given below, we really detect the paramagnetic-sinusoidal phase transition instead of the paramagnetic-$\langle 2 \rangle$ phase. This implies that one must consider the possible "ground states" of the sinusoidal phase rather than the ground states of the $\langle 2 \rangle$ phase. However, such a calculation requires very long chains and sophisticated choices of N and N'. We believe the choice of N and N' as integral multiples of four to be acceptable for our purpose.

[16] S. Redner, J. Stat. Phys. <u>25</u>, 15 (1981).

[17] The critical exponent α is expected to be $\frac{1}{2}$ from the sinus side only.

[18] H. A. Kramers and G. H. Wannier, Phys. Rev. <u>60</u>, 252 (1941).

[19] M. E. Fisher and H. N. Barber, Phys. Rev. Lett. <u>28</u>, 1516 (1972).

[20] L. P. Kadanoff, Physics (N.Y.) <u>2</u>, 263 (1966).

[21] For a review, see K. G. Wilson and J. Kogut, Phys. Rep. <u>120</u>, 76 (1974).

[22] T. Niemeijer and J. M. J. van Leeuwen, Physica (Utrecht) <u>71</u>, 17 (1974).

[23] Z. Friedman, Phys. Rev. Lett. <u>36</u>, 1326 (1976); K. Subbarao, Phys. Rev. Lett. <u>37</u>, 1712 (1976).

[24] S. Drell, M. Weinstein, and S. Yankielowitz, Phys. Rev. D <u>14</u>, 487 (1976). For a recent review, see W. J. Caspers, Phys. Rep. <u>63C</u>, 223 (1980).

[25] See C. J. Hamer and M. N. Barber, J. Phys. A <u>14</u>, 241 (1981), and references therein.

[26] Such calculations have been performed recently for models with Ising symmetry [C. J. Hamer and M. N. Barber, J. Phys. A <u>14</u>, 241 (1981)], hard-core lattice systems [Zoltán Rácz, Phys. Rev. B <u>21</u>, 4012 (1980), and references therein], two-dimensional Potts models [M. P. Nightingale and H. W. J. Blöte, Physica (Utrecht) <u>104A</u>, 352 (1980)], two-dimensional $O(2)$ and $O(3)$ models [C. J. Hamer and M. N. Barber, J. Phys. A <u>14</u>, 259 (1981)], lattice gauge systems [H. H. Roomany and H. W. Wyld, Phys. Rev. B <u>23</u>, 1357 (1981)], etc.

[27] H. J. Schultz, Phys. Rev. B <u>22</u>, 5274 (1980) and Ref. 8.